CORE
Metadata, citation and similar papers at core.ac.uk
Provided by IntechOpen

We are IntechOpen, the world's leading publisher of Open Access books Built by scientists, for scientists

4,800
Open access books available

122,000
International authors and editors

135M
Downloads

Our authors are among the

154
Countries delivered to

TOP 1%
most cited scientists

12.2%
Contributors from top 500 universities

WEB OF SCIENCE™

Selection of our books indexed in the Book Citation Index in Web of Science™ Core Collection (BKCI)

Interested in publishing with us?
Contact book.department@intechopen.com

Numbers displayed above are based on latest data collected.
For more information visit www.intechopen.com

Chapter 8

Mineralogical Characterization of Chalcopyrite Bioleaching

E.R. Mejía, J.D. Ospina, L. Osorno, M.A. Márquez and A.L. Morales

Additional information is available at the end of the chapter

http://dx.doi.org/10.5772/59489

1. Introduction

Chalcopyrite ($CuFeS_2$) is the most important copper ore, comprising approximately 70% of copper reserves in the world [1,2]. In metallurgical applications, chalcopyrite is mainly subjected to pyrometallurgy treatment after concentration by a flotation process [3,4]. The interest in bio-hydrometallurgy has increased recently in order to minimize the sulfur dioxide emissions, and to reduce energy consumption [5-9]. However, the chalcopyrite copper leaching rate is slower than other copper minerals such as chalcocite (Cu_2S), covellite (CuS), and bornite (Cu_5FeS_4) [10]. Initial rapid leaching rates decline with time, and bioleaching processes release only part of the copper [11]due to so-called passivation reactions at the mineral surfaces [12, 13]. After almost a century of research into the mechanisms of chalcopyrite dissolution in ferric media, there is a consensus with respect to the formation of a passivating film on the surface [3, 11-16]. Despite this, the nature of this film remains unknown, although it has been postulated that it must have low porosity and be a bad electricity conductor (Córdoba *et al.*, 2008a). Various models were describing the mass transfer diffusion and chemical reactions on the chalcopyrite surface. Those models have been proposed to explain the nature and composition of the passivation film that causes slow oxidation of the chalcopyrite: (I) metal-deficient sulfides, (II) elemental sulfur-S^o, (III) polysulfides-XS_n, and (vi) jarosite-$XFe_3(SO_4)_2(OH)_6$ [4, 11-17].

Klauber (2008) [8] reviewed the chemical characteristics of the surface layer of chalcopyrite leached with ferric sulfate and suggested passivation candidates including metal-deficient sulfides and elemental sulfur-S^o. This author suggested that the metal-deficient sulfide is formed by non-stoichiometric dissolution of sulfides based on analytical evidence. Parker *et al.* (2003) [11] used XPS analysis to detect elemental sulfur, sulfate, and disulfide phases in the

INTECH
open science | open minds

© 2015 The Author(s). Licensee InTech. This chapter is distributed under the terms of the Creative Commons Attribution License (http://creativecommons.org/licenses/by/3.0), which permits unrestricted use, distribution, and eproduction in any medium, provided the original work is properly cited.

solid form in chalcopyrite bioleaching experiments. Additionally, chalcopyrite bioleaching results in the dissolution of iron, which potentially leads to precipitation of Fe^{3+} hydroxysulfates such as jarosite [11]. Under these conditions, chalcopyrite leaching may involve iron-deficient secondary minerals and intermediates [19].

These studies agreed that the jarosite precipitation is linked to chalcopyrite passivation. These different theories require substantial further research. It is, therefore, crucial to tackle the issue from different angles in an attempt to understand the nature of the recalcitrant chalcopyrite.

Moreover, mineralogical characterization of the products in different types of beneficiation processes, called "process mineralogy," has been performed as a fundamental piece of the planning, optimizing, and monitoring of different minerals [5, 20]. In this way, an appropriate understanding of the mineralogy in the chalcopyrite and its transformation is essential to understanding the passivation mechanism [21]. This type of research can be turned quite complicated due to factors like fine size of particles, low crystallinity, a small proportion of mineral phases, and nature of ore minerals in the various steps of the process. Due to these features it is necessary to use different complementary analytical techniques like electron microscopes, electron microprobe, X-ray diffractometers and spectrometric methods [22, 23].

The primary objective of this research is to characterize the mineral phases generated in the bioleaching process of chalcopyrite and to understand the evolution or transformation of these phases to elucidate its influence on chalcopyrite passivation of the process.

2. Material and methods

2.1. Mineral

All experiments were carried out using a natural chalcopyrite sample from "La Primavera" Mine (La Cruzada Segovia, Antioquia, Colombia). The mineral was subjected to crushing and milling processes followed by gravimetric separation in a Wilfley table. Afterward, manual concentration was performed under stereographic microscopy. The mineral composition of the sample measured by countdown points was 85.23% chalcopyrite ($CuFeS_2$), 1.27% quartz (SiO_2), 1.69% covellite (CuS), 2.53% sphalerite, and 3.37% molybdenite (MoS_2). The mineral was milled using an agate mortar. This guaranteed size, pass through 200 Tyler mesh (~75μm), and the mineral was then sterilized in a furnace for 90 min at 80 °C.

2.2. Bioleaching experiments

Acidithiobacillus ferrooxidans ATCC 23270 bacterial strains was employed in the bioleaching experiments. The microorganisms were previously grown in T&K medium ($(NH_4)SO_4$: 0.5g/L; $MgSO_4.7H_2O$: 0.5g/L; K_2HPO_4: 0.5g/L) [24, 25]. By successive replacement of the ferrous sulfate with chalcopyrite. The medium was acidified to pH 1.8 using H_2SO_4. The flasks were sterilized by autoclaving for 20 min, 120°C at 18 psi. The experiment was inoculated with *A. ferrooxidans* 10% (v/v) with 10^7 cel/ml. The experiments were carried out for 30 days in 500-mL

flasks containing 300 mL medium with 10% (w/v) chalcopyrite. Those were shaking at 180 rpm and 30ºC. All conditions were duplicated, and the respective abiotic control was included.

2.3. Chemical analysis

Measurements of pH (HACH HQ40d multi PHC30103) and redox potential (Shot Handylab 1 Pt 6880) (reference electrode $Ag^0/AgCl$) were performed *in situ* every day. Samples were aseptically withdrawn from the flasks after 24 h and then every five days for mineralogical and chemical analysis. The samples were separated in a DIAMOND IEC DIVISION centrifuge for 15 min at 3000 rpm. Iron and sulfate concentrations were measured with an UV-visible GENESYS™ 10 spectrophotometer. The methods employed were 3500-FeD (O-phenantroline) for total iron according to the Standard Methods for water analysis[26].

2.4. Mineralogical analysis

Combinations of analytical techniques were used in the mineralogical sample characterization. The Fourier transform infrared (FTIR) spectra for the solid samples were recorded in an FTIR Spectrophotometer Shimadzu Advantage 8400 using KBr pellets in transmission mode. A sample of the KBr mixture at a 1:200 ratio was used. A total of 20 scans with a spectral resolution of 4 cm^{-1}, a range of 400–4000 cm^{-1}, and Happ-Henzel correction were used. The biooxidation samples were mounted in epoxy resin and polished with sequentially finer SiC grit paper and a final polish with 0.05-μm alumina powder. Polished section analysis was performed with JEOL JSM 5910 LV scanning electron microscopy (SEM) in backscattering electron mode and an energy-dispersive X-ray spectroscopy detector (EDX) (Oxford Instrument) using a beam voltage of 18 kV.

X-ray diffraction (XRD) analyses of the samples were conducted in a Bruker D8ADVANCE diffractometer with Cu λ=1.5406 Å radiation generated at 35 kV and 30 mA. XRD data were obtained using a computer-controlled XRD Panalytical X'Pert Pro MPD. The samples collected for mineralogical studies have a statistical representation and the analyses performed by different techniques and on different grains for the same mineral give validity to the results.

3. Results

3.1. Chalcopyrite leaching experiment

Chalcopyrite oxidation in the inoculated culture presented a low pH (2.1), while the control pH was 2.8. Redox potencial increased from 330 mV until 580 mV. The abiotic control did not change in the time (180 mV). The dissolution of total Fe (Fig. 1) presented continue increase in the time showed a maximum value at 15th day (8182.25 ppm) and then decreased and stay invariant until 7251.44 ppm, abiotic control did not show a significant changes in the time (780,12 ppm).

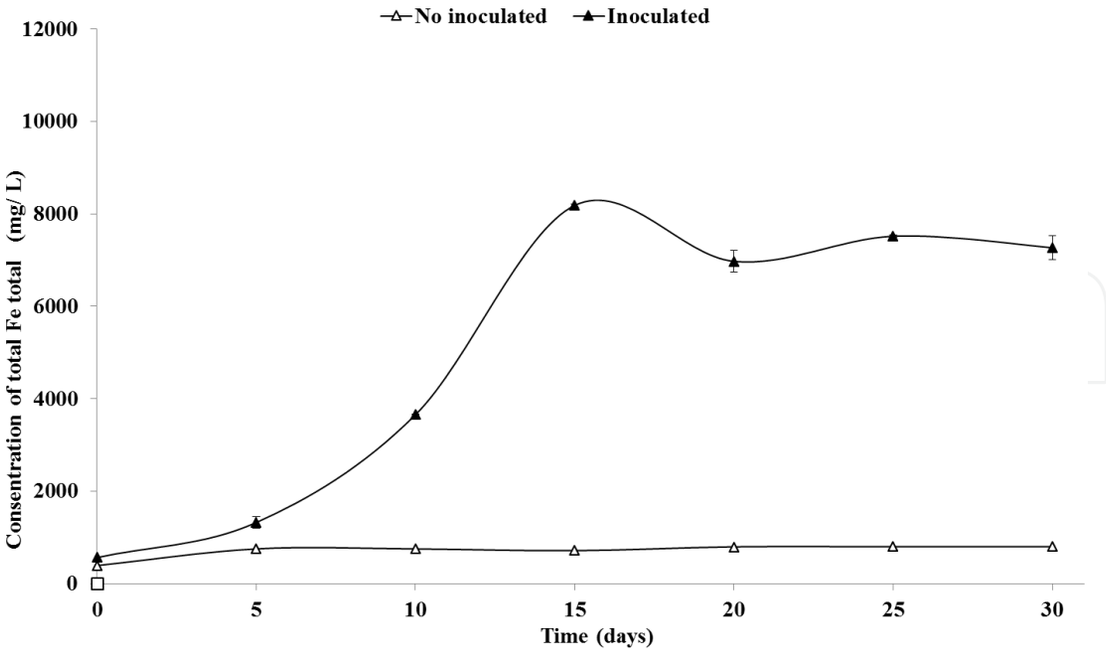

Figure 1. Concentration of total Fe (mg/L) in the Time (Day).

The concentration of SO_4^{2-} reached its maximum value at 15th day (50200 ppm) after this day it was decreased until 25600 ppm (Fig 2). The no inoculated flask did not present considerable variation in the time, and those had a significant difference compared with an inoculated test.

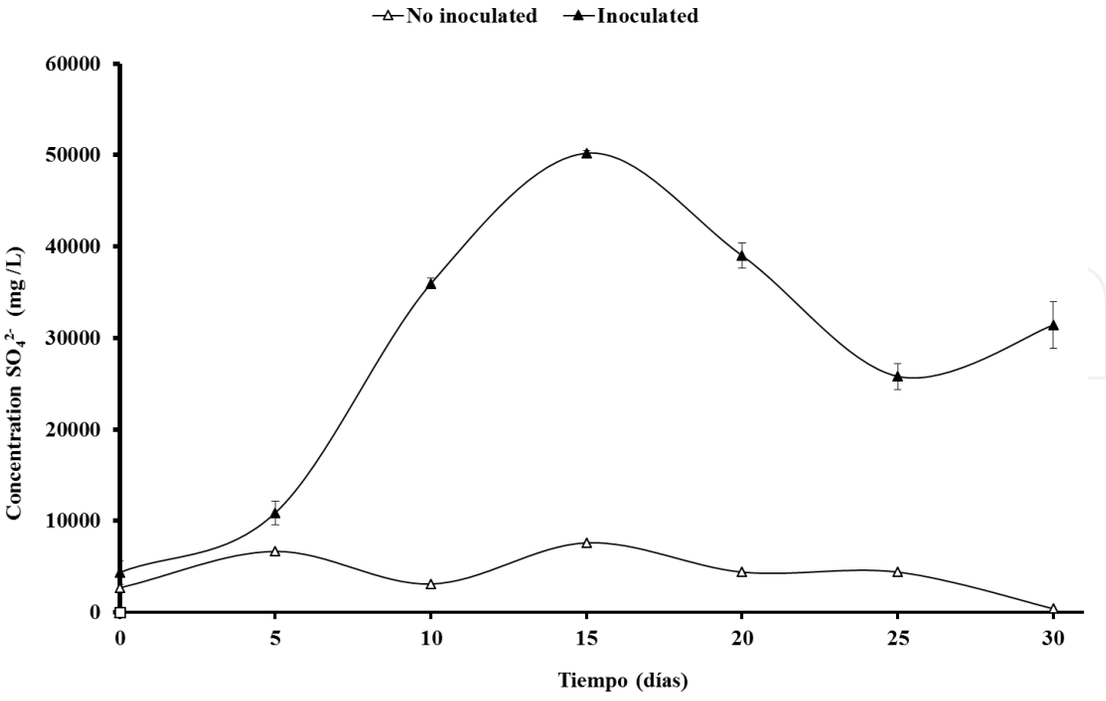

Figure 2. Concentration of sulphate (mg/L) in the Time (day).

http://dx.doi.org/10.5772/59489

Copper extraction was 35.45%; this dissolution was growing at 15th day next stabilized in the time. Less than 6% of Cu was solubilized in the chemical controls (Fig. 3).

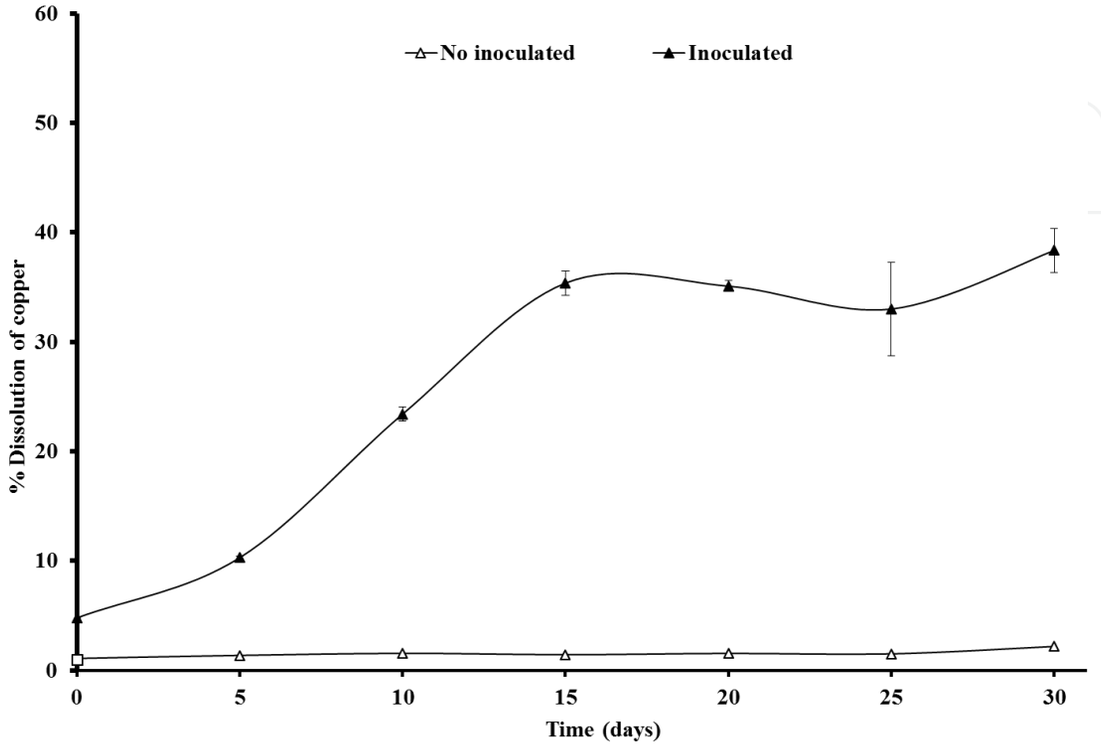

Figure 3. Copper dissolution (%) in the Time (Day).

3.2. Mineralogical analysis

3.2.1. FTIR measurements

Results obtained by FTIR (Fig 4) showed that the predominant mineral phase present was jarosite, which was confirmed by the presence of the ν_3 band (anti-symmetric stretching triply degenerate vibration) at 1190 cm^{-1}, 1085 cm^{-1}, and 1008 cm^{-1}, ν_4 band (deformation vibration) at 629 cm^{-1}, and ν_2 bands (deformation vibration doubly degenerate) at 513 cm-^{1} and 470 cm^{-1} [19, 21, 27, 28]. There was also absorption at 740 cm^{-1}, 870 cm^{-1}, and 1414 cm^{-1}, which may correspond to ν_3 of NH_4^+ in the ammonium jarosite [19]. In addition, typical bands of quartz at 798 cm^{-1}, 779 cm^{-1}, and 694 cm^{-1} could be observed [29] as well as the hydroxyl groups at 3400 cm^{-1} and water at 1640 cm^{-1} of the jarosite mineral [28, 30]. Bands around 2935 cm^{-1} related to the total carbon present on the cell surface showed a permanent increase [31-33]. The samples did not show a significant difference during the first five days, but between the 5th and the 10th day, the width and intensity of the jarosite bands significantly increased. After this point, the band increases in the samples were very slow. FTIR of uninoculated samples for all tests showed a spectrum with little variation compared with the unleashed sample.

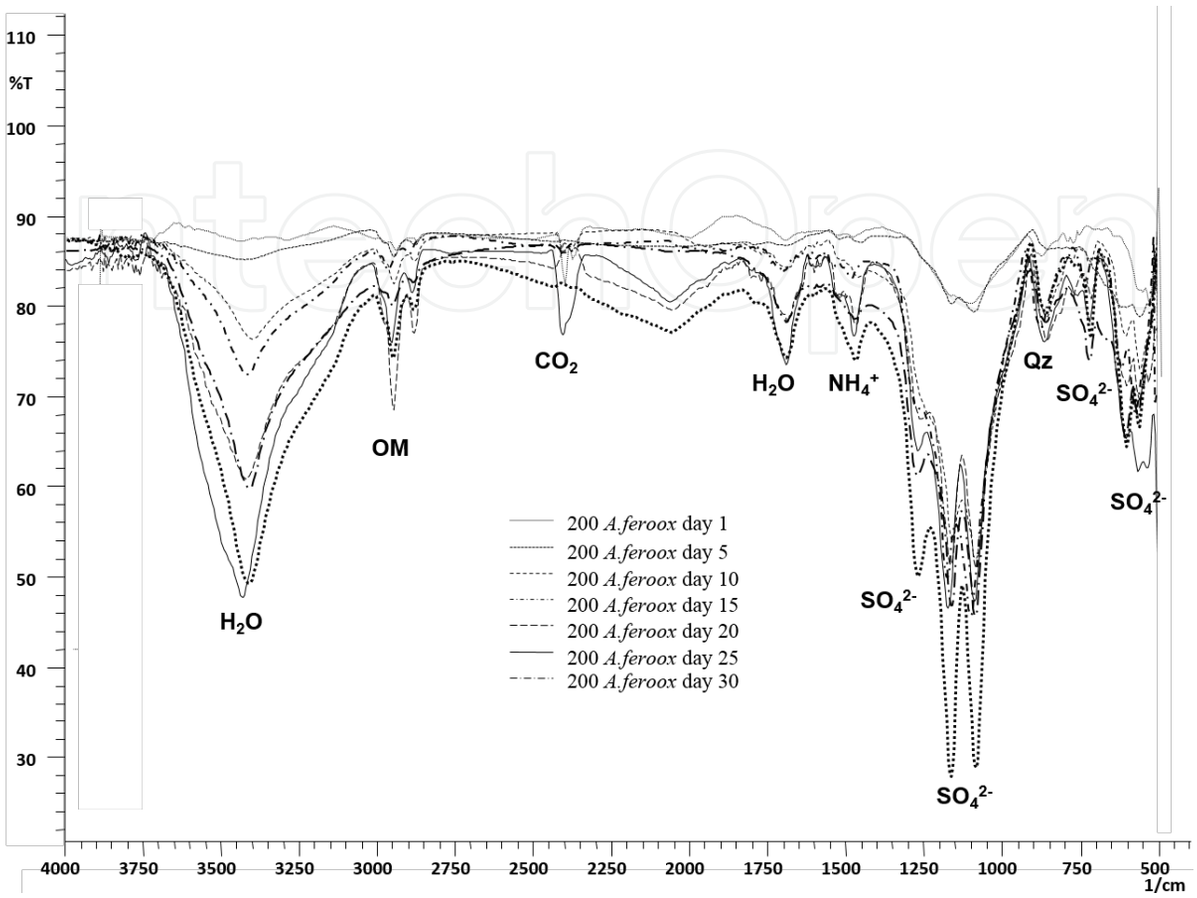

Figure 4. Fourier transforms infrared spectra of solid residues after bioleaching of chalcopyrite. H_2O (water), OM (organic matter), CO_2 (Carbon dioxide), NH_4^+(ammonium in jarosite), SO_4^{2-} (sulphate in jarosite) and Qz (quartz).

3.2.2. SEM/EDX analysis

SEM images of uninoculated samples for all tests (Fig. 5) showed surfaces with few alterations such as isolated cracks. These alterations were interpreted as mineral genetic defects. The grains had well-defined edges. EDX analysis of the grains showed the chalcopyrite's stoichiometric composition (Fig. 6). The morphology of the grains exposed to bacteria is illustrated in Figs. 7. All the samples show typical corrosion features such as pits, grooves, and gulfs on the surfaces of the chalcopyrite grains (Figs. 7) that increased from the edge of the grain toward the core. These characteristics were observable the first day of the process and became more evident with time. EDX also characterized an aggregate containing S, O, and Fe (Fig.6). Average pit size and pitting density on the surface increased with reaction time. After 15 days, the surface pitting was extensive, resulting in discrete euhedral and elongated pits and grooves (Fig. 7). The formation of jarosite aggregates increased with time and sharply increased until the end of the process. Moreover, some grains showed a partial jarosite film covering the chalcopyrite grains since the first day of the process (Fig. 7)

http://dx.doi.org/10.5772/59489

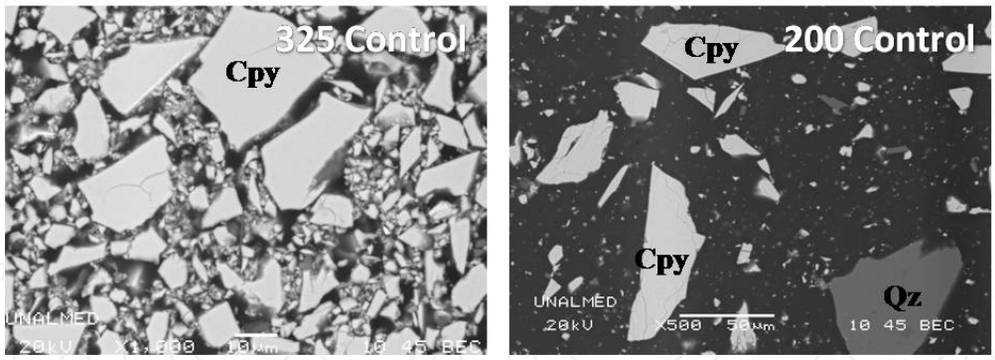

Figure 5. Scanning electron microscopy micrographs of uninoculated residues after chalcopyrite bioleaching. Cpy, chalcopyrite; Qz, quartz. After 30 days.

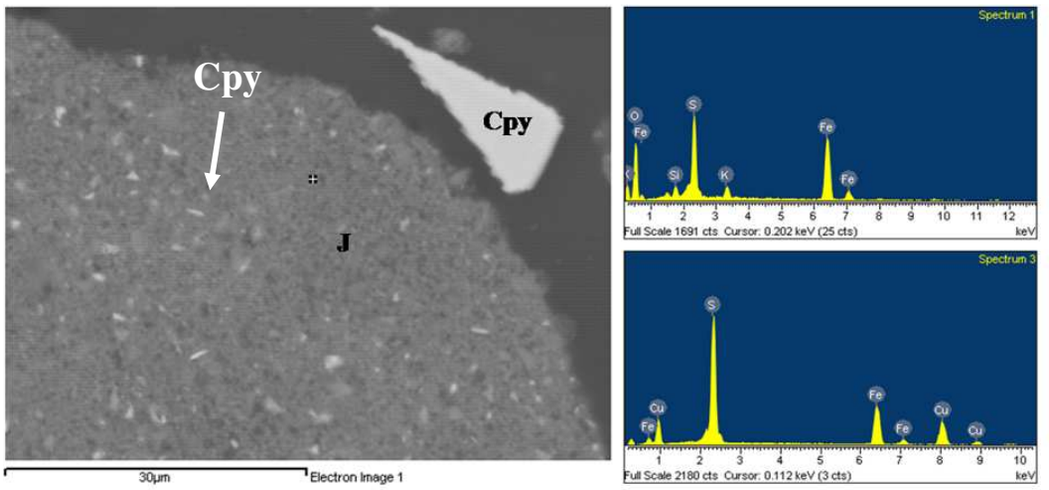

Element	Weight%	Atomic%
O K	31.99	57.25
Si K	2.20	2.25
S K	15.98	14.27
K K	3.10	2.27
Fe K	46.73	23.96

Element	Weight%	Atomic%
S K	32,6	47,5
Fe K	31,19	26,05
Cu K	36,35	26.60

Figure 6. Scanning electron microscopy/energy dispersive X-ray spectroscopy micrograph and analysis of the residues after bioleaching with *A. ferrooxidans* of chalcopyrite. Cpy, chalcopyrite; J, jarosite.

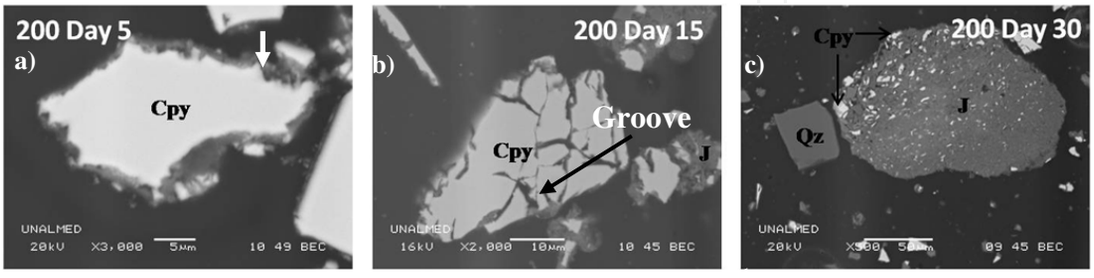

Figure 7. Scanning electron microscopy micrographs of the residues after chalcopyrite bioleaching with *A. ferrooxidans*. Cpy, chalcopyrite; J, jarosite; and Qz, quartz. a) day 5, b) day 15 and c) day 30.

3.2.3. XRD measurements

According to the XRD initial qualitative analysis, were founding that the primary mineral phase present in the samples was chalcopyrite with small quantities of quartz, molybdenite, covellite, chlorite and wollastonite (Fig. 8). From the result obtained by XRD spectra of bioleached samples (Fig. 9), the most important identified minerals were:

i. as the principal products of the bacterial oxidation process: (a) ammonium jarosite, as preponderant phase and covellite in minor quantities and (b) Wollastonite was dissolved at the beginning of the process.

ii. as mineral phases resistant to the bioxidation process: (a) Chalcopyrite, as the primary sulfide, present in every sample, (b) Minor quantities of pyrite and (c) different types of silicates like quartz, chlorite and muscovite.

Otherwise, mineralogical evolution of the mineral phases consists of a gradual reduction of molybdenite and chalcopyrite peaks and the appearance of ammonium jarosite and covellite. XRD for uninoculated controls did not show change in the time (Fig. 10).

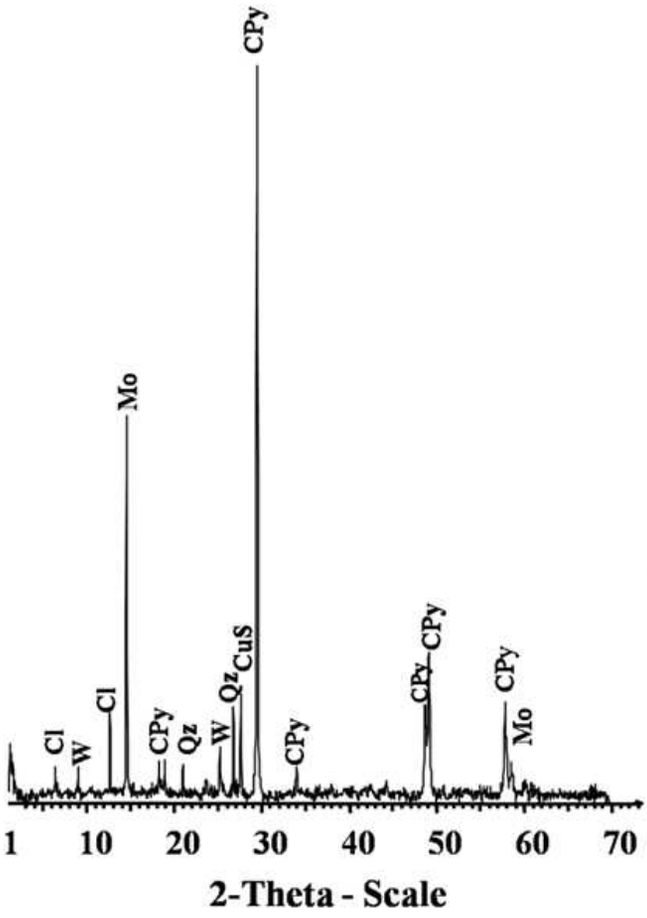

Figure 8. X-ray diffraction spectra for chalcopyrite of sample before the bioleaching process (CPy, chalcopyrite; Qz, quartz; Mo, molybdenite; W, wollastonite; Cl, chlorite; CuS, covellite.

http://dx.doi.org/10.5772/59489

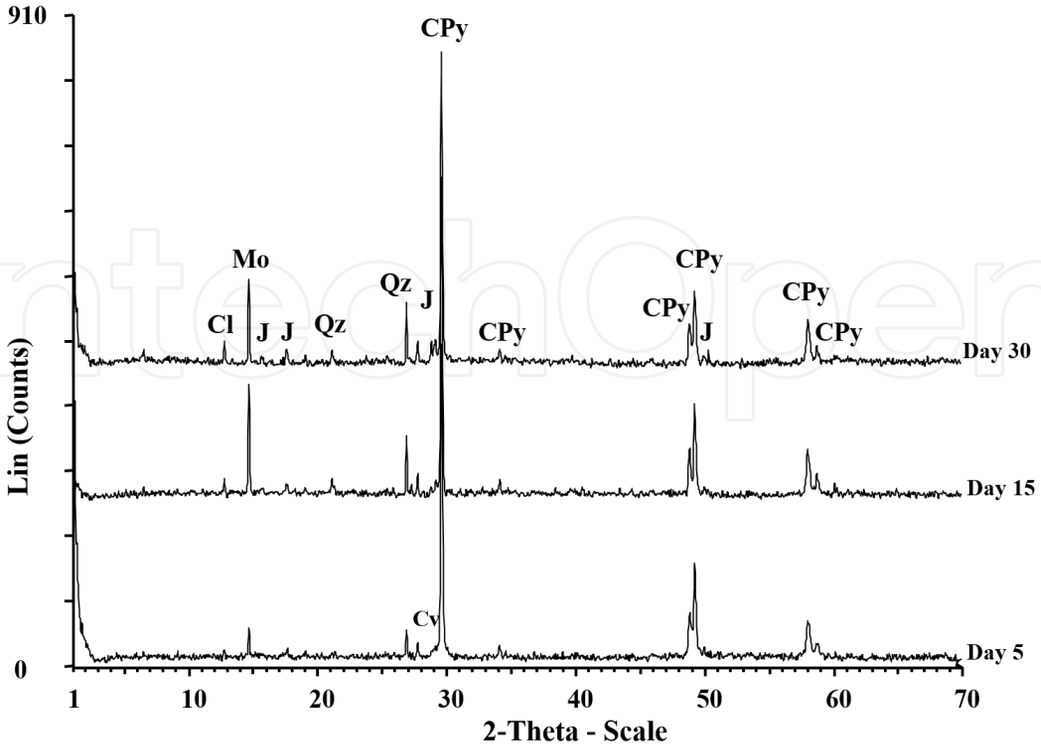

Figure 9. X-ray diffraction spectra of chalcopyrite during the bioleaching process in the 5, 15 and 30 days. (CPy, chalcopyrite; Qz, quartz; Mo, molybdenite; W, wollastonite; Cl, chlorite; J, jarosite; Cv, covellite).

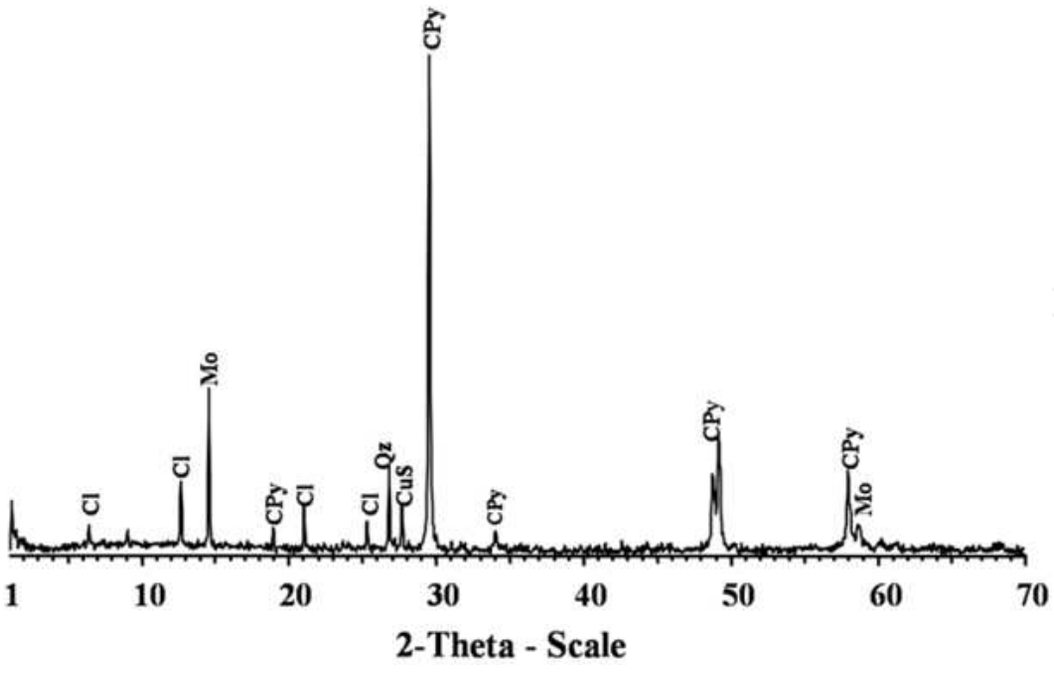

Figure 10. X-ray diffractograms of uninoculated samples after 30 days of the process. (CPy, chalcopyrite; Qz, quartz; Mo, molybdenite; Cl, chlorite; CuS, covellite).

4. Discussion

4.1. Chalcopyrite leaching experiment

As previously stated, it is possible to conclude that the chalcopyrite bioleaching process was passivated. The results suggest that a low level of Fe^{3+} is favorable for Cu lixiviation since the copper release slowed at high Fe^{3+} concentration. Chemical analysis showed that around the 15th day, the system had a flat ferrous ion concentration, high ferric ion concentration, increased redox potential, and decreased copper dissolution. Hiroyoshi *et al.* (2001) [10] found that when the concentration of ferrous and cupric ions is low in the system, the overall reaction of chalcopyrite leaching is controlled by ferric ions and the copper extraction rate is slower. This could explain what happened after at 15 days the release of copper occurs more slowly. Furthermore, ferrous ions promoted chalcopyrite bioleaching below the "critical" potential, in this case around of 430 mV, which caused enhanced copper removal on days 1–15. In the higher potential area (days 16–30), the release of copper was smaller than that in the lower-potential region because there might not have been enough ferrous ion to promote chalcopyrite bioleaching. The present findings agree with those of previous works [3,4, 10, 34, 35]. The hypotheses in these works were that the chalcopyrite dissolution was catalyzed by the ferrous ion according to the following reactions (1-3):

$$CuFeS_2 + 4H^+ + O_2 \rightarrow Cu^{2+} + 2S^0 + Fe^{2+} + 2H_2O \quad (1)$$

$$CuFeS_2 + 3Cu^{2+} + 3Fe^{2+} \rightarrow 2Cu_2S + 4Fe^{3+} \quad (2)$$

$$2Cu_2S + 8Fe^{3+} \rightarrow 4Cu^{2+} + 8Fe^{2+} + 2S^0 \quad (3)$$

These researchers found that the inhibition of chalcopyrite bioleaching by mesophilic microorganisms is due to bacterial consumption of ferrous ion. In these reactions, the role of microorganisms such as *A. ferrooxidans* was not evident, and the copper dissolution was a purely chemical process. However, in the present study, we observed that *A. ferrooxidans* plays a fundamental role in the copper dissolution, as can be seen in the chemical controls where dissolution practically fails to occur.

Nevertheless, some researchers have found that copper release is favored at high Fe^{3+} concentrations, where this ion contributes to the overall efficiency of the chalcopyrite leaching in which ferric ions acts as oxidizers, producing elemental sulfur according to the following reaction (4) [11, 16, 3-39].

$$CuFeS_2 + 4Fe^{3+} \rightarrow 5Fe^{2+} + Cu^{2+} + 2S° \quad (4)$$

4.2. Mineralogical analysis

From the results previously outlined, it is possible to conclude that the leaching process the silicates did not present detectable changes, demonstrating refractoriness to it. Jarosite is the most abundant mineral phase as product of the bacterial leaching of chalcopyrite. There is a predominance of the ammonic component in the jarosite. The generation of jarosite in bacterial systems has been already documented in the literature [21]. [40] Produced jarosite using *A. ferrooxidans* and demonstrated the preference in the incorporation of K^+ and NH_4^+ in the jarosite in this system. Ammonium in the jarosite was incorporated probably from compounds used as nutrients in these processes.

Jarosite phase could be considered as the unfavorable phase because its presence apparently would passivate the copper release [5, 10, 11, 16, 34-38]. The jarosite formation was more marked from 15th day onward, when the system showed a lower concentration of ferrous ion, a higher concentration of ferric ion, increased redox potential, and a high concentration of SO_4^{2-} in the solution. Jarosite formation was favored when redox potentials increased above the critical value (430 mV) around the 15th day, favoring the hydrolysis of ferric ion, promoting jarosite precipitation, and possibly generating chalcopyrite passivation [5]. The formation of jarosite was confirmed by FTIR spectra, which showed permanent increases in the typical bands.

The sharp increase of jarosite bands on the 15th day and its further slow increase was consistent with the observed chemical data. It is important to note the jarosite bands more defined with the time. It could involve a crystallinity increase in the jarosite structure. On the other hand, the increase of the band at 2935 cm^{-1} was possibly due to an increase in bacterial population, indicating bacterial activity, which cannot detected by other characterization techniques [33]. Moreover, the NH_4 bands increased and were clearer with the time. It could indicate the NH_4 was gradually incorporating into the jarosite structure. Ammonium in the jarosite incorporated probably from compounds of ammonium, which are used as nutrients in this process, since it is the case of the ammonium sulfate added in T&K as source of energy [21]. In this way, if the microorganism did not have a NH_4 as source of energy they could decrease its activity.

Furthermore, SEM analysis showed that chalcopyrite dissolution, in the presence of these microorganisms, occurred on the surface due to the presence of roughening of the grains and the formation of dissolution pits, both of which increase with time. The pH reigning in the test and the high levels of Fe^{3+} and SO_4^{2-} could generate system instability, favoring the precipitation and nucleation of jarosite agglomerating on small chalcopyrite particles, increasing after the 10th day and forming a non-uniform film on the largest chalcopyrite grains. Jarosite precipitation was indicated by breakage in the solubility limit of iron and sulfates in the solution, which could be mitigated by reduced levels of sulfates in the medium [1, 5, 30, 34]

On the other hand, XRD analysis (Figs. 9) indicated that jarosite formed at the expense of chalcopyrite dissolution. Moreover, XRD spectrum showed a covellita formation at the expense of chalcopyrite dissolution. In contrast, the chalcopyrite in the control reaction system remained visually unaltered. Nevertheless, the dissolution of minority phases as molybdenite,

wollastonite, and chlorite was observed. This mineralogical analysis showed the predominance of the galvanic effect, where lower-potential molybdenite dissolves in contact with chalcopyrite [41, 42].

Moreover, chlorite and wollastonite are soluble in acidic environments [5], and small quantities of the Cl^- ion are not toxic to the bacterial population [43]. The increased relative abundance in the process could indicate a reduced ratio of chalcopyrite to covellite and, therefore, confirms the hypotheses raised by Hiroyoshi *et al.* [44-48], where the ferrous ions promoted chalcopyrite leaching, favoring the reduction of chalcopyrite to covellite and the simultaneously oxidation of this mineral. However, in this case, the ferrous ions apparently induced the reduction of chalcopyrite to covellite and the simultaneous oxidation. The hypothesis of this work was that the chalcopyrite dissolution was initially catalyzed by the ferrous ion according to the following reactions (5-7):

$$CuFeS_2 + 4H^+ + O_2 \rightarrow Cu^{2+} + 2S^0 + Fe^{2+} + 2H_2O \quad (5)$$

$$CuFeS_2 + Cu^{2+} + Fe^{2+} \rightarrow 2CuS + 2Fe^{3+} \quad (6)$$

$$CuS + Fe^{3+} \rightarrow Cu^{2+} + Fe^{2+} + S^0 \quad (7)$$

Finally, it was possible to define the mechanisms from bacterial leaching of chalcopyrite is according figure 11:

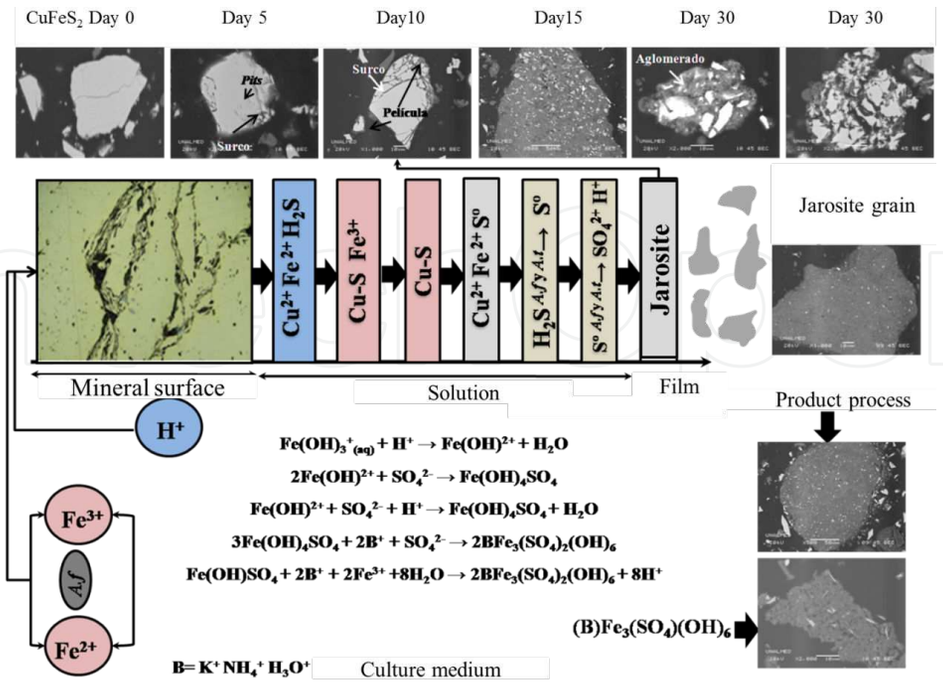

Figure 11. Chalcopyrite bioleaching mechanism.

http://dx.doi.org/10.5772/59489

5. Conclusions

The characterization the mineral phases generated in the bioleaching process of chalcopyrite for *A. ferrooxidans* allowed understanding the transformation of these phases in the process chalcopyrite passivation. We showed that chalcopyrite bioleaching is not a typical bioprocess because faster and greater extractions resulted when the leaching was performed at low redox potential values. In this case, the ferrous ions apparently favored the reduction of chalcopyrite to CuS and the simultaneous oxidation of this newly formed phase, increasing the release of copper. A high concentration of Fe^{3+} produces chemical instability in the process, favoring the precipitation of the jarosite principal phase formed in the processes. This phenomenon could be responsible for inhibiting chalcopyrite bioleaching. The results suggest that the mineral dissolution rate was affected by jarosite formation. This mineral may limit the diffusion of ions through the chalcopyrite surface and the access of the leaching solution. The bacteria A. ferrooxidans play an important role in the chalcopyrite bioleaching.

Acknowledgements

The authors would like to thank the San Buenaventura University, Program of Biotechnology of Colciencias, Colombia, Laboratory of Biomineralogy of the National University of Colombia, the Laboratory of Mineralurgy, University of Antioquia, and the Laboratory of Coal, National University of Colombia, University Pascual Bravo institution by the economic support in the mineralogical characterization of samples.

Author details

E.R. Mejía[1,3*], J.D. Ospina[2], L. Osorno[3], M.A. Márquez[3] and A.L. Morales[4]

*Address all correspondence to: erika.mejia@usbmed.edu.co

1 Universidad San Buenaventura, sede Medellín, Facultad de artes integradas, Grupo de Investigación Hombre, Proyecto y Ciudad, Colombia

2 Institución Universitaria Pascual, Facultad de Ingeniería. Grupo de Investigación e Innovación Ambiental, Colombia

3 Universidad Nacional de Colombia, Medellín, Facultad de Ciencias y Facultad de Minas. Grupos de Investigación en Microbiología del Suelo y Mineralogía Aplicada y Bioprocesos, Colombia

4 Grupo de Estado Sólido, Instituto de Física, Universidad de Antioquia, Medellín, Colombia

References

[1] Dutrizac, J.E. 1981. The dissolution of chalcopyrite in ferric sulfate and ferric chloride media. Met. Trans. B. 12B: 371-378.

[2] Rivadeneira, J. 2006. Introduction. Mining innovation in Latin America Report. Publication via on-line (http://www.mininginnovation.cl/content.htm). Santiago, Chile, pp. 6–7.

[3] Córdoba, E.M., Muñoz, J.A., Blázquez, M.L., González, F., Ballester A. 2008a. Leaching of chalcopyrite with ferric ion. Part I: General aspects Hydrometallurgy. 93 81.

[4] Córdoba, E.M., Muñoz, J.A., Blázquez, M.L., González, F., Ballester A. 2008b. Leaching of chalcopyrite with ferric ion. Part IV: The role of redoxpotential in the presence of mesophilic and thermophilic bacteria. Hydrometallurgy. 93 88.

[5] Marsden, J., House, I. 1992. The Chemistry of Gold Extraction. Ellis Horwood, New York, 579.

[6] Brierley, J.A., Luinstra, L. Biooxidation-heap concept for pretreatment of refractory gold ore. In: Biohydrometallurgical Technologies, A.E. Torma, J.E. Wey & V.L. Lakshmanan Eds., The Minerals, Metals & Materials Society, pp. 437-448. 1993.

[7] Hsu, C.H., Roger, G.H. 1995. Bacterial leaching of zinc and copper from mining wastes. Hydrometallurgy. 37 169-179

[8] Watling, H.R. 2006. The bioleaching of sulphide minerals with emphasis on copper sulphides—a review. Hydrometallurgy. 84 81–108.

[9] Al-Harahsheh, M., Kingman, S., Rutten, F., Briggs, D. 2006. ToF-SIMS and SEM study on the preferential oxidation of chalcopyrite. International Journal of Mineral Processing. 80 2-4.

[10] Hiroyoshi, N., Miki, H., Hirajima, T., Tsunekawa, M. 2000. A model for ferrous-promoted chalcopyrite leaching. Hydrometallurgy. 57 31– 38.

[11] Yin, Q., Kelsall, G.H., Vaughan, D.J., England, K.E.R. 1995. Atmospheric and electrochemical oxidation of the surface of chalcopyrite (CuFeS2). Geochimica et Cosmochimica Acta. 59 1091-1100.

[12] Hackl, R.P. Dreisinger, D.B. Peters, E. King J.A. 1995. Passivation of chalcopyrite during oxidative leaching in sulfate media. Hydrometallurgy. 39 1-3,25-48.

[13] Schippers A., Sand W. 1999. Bacterial leaching of metal sulfides proceeds by two indirect mechanisms via thiosulfate or via polysulfides and sulfur. Applied Environmental Microbiology. 65 1, 319-321.

[14] Mikhlin, Y.L., Tomashevich, Y.V.,. Asanov, I.P., Okotrub, A.V., Varnek, V.A., Vyalikh, D.V. 2004. Spectroscopic and electrochemical characterization of the surface layers of chalcopyrite reacted in acidic solutions, Applied Surface Science 225 395–409.

[15] Bevilaqua, D., Leite, A.L.L.C., Garcia Jr., O., Tuovinen, O.H. 2002. Oxidation of chalcopyrite by *Acidithiobacillus ferrooxidans* and *Acidithiobacillus thiooxidans* in shake flasks. Process Biochemistry. 38, 587-592.

[16] Harmer, S.L., Thomas, J.E., Fornasiero, D., Gerson, A.R. 2006. The evolution of surface layers formed during chalcopyrite leaching. Geochimica et Cosmochimica Acta 70 4392–4402.

[17] Klauber, C. 2008. A critical review of the surface chemistry of acidic ferric sulphate dissolution of chalcopyrite with regards to hindered dissolution. Int. J. Miner. Process. 86 1–17.

[18] Harvey, P.I., Crundwell, F.K. 1996. The effect of As(III) on the growth of *Thiobacillus ferrooxidans* in an electrolytic cell under controlled redox potentials. Minerals Engineering. 9 10 1059-1068.

[19] Petruk, W. 2000. Applied mineralogy in the mining industry. Elsevier. Ottawa, Ontario, Canada.

[20] Márquez, M.A., Gaspar, J.C., Bessler, K.E., Magela G. 2006. Process mineralogy of bacterial oxidized gold ore in São Bento Mine (Brasil). Hydrometallurgy. 83 1-4 114-123.

[21] E. Mejía, J. D. Ospina, M. A. Márquez and A. L. Morales (2012). Bioleaching of Galena (PbS), Fourier Transform-Materials Analysis, Dr Salih Salih (Ed.), ISBN: 978-953-51-0594-7, InTech, Available from: http://www.intechopen.com/books/fourier-transform-materials-analysis/bioleaching-of-galena-pbs-

[22] Márquez, M.A., Ospina, J.D.; Mejía, E; Osorno, B.L.; Morales, A.L. (2013) Estudio μraman de la oxidación superficial de la pirita (Fes2), Calcopirita (CuFeS2) por *Acidithiobacillus ferrooxidans*. Rev. ACCEFYN. ISSN: 0370-390, Vol 14. Pp. 373-380.

[23] Tuovinen O., Kelly D. 1973. Studies on the growth of *Thiobacillus ferrooxidans*. Arch. Microbiol. 88: p 285–298.

[24] Fowler T.A., Holmes P.R., Crundwell F.K. 1999. Mechanism of pyrite dissolution in the presence of *Thiobacillus ferrooxidans*. Applied And Environmental Microbiology. 65: p 2987–2993.

[25] Lenore, S., Clesceri, A. E., Greenberg Eaton, A.D. 1999. Standard Methods for the Examination of Water and Wastewater. American Public Health Association, American Water Works Association, Water Environment Federation. 20Th edition.

[26] Chernyshova, I.V. 2003.An in situ FTIR of galena and pyrite oxidation in aqueous solution. 558. 83-98.Da Silva, G., Lastra, M. R., Budden, J. R. 2003. Electrochemical

passivation of sphalerite during bacterial oxidation in the presence of galena. Minerals Engineering. 16 199 – 203.

[27] Gunneriusson, L., Åke Sandström, Holmgren, A., Kuzmann, E., Kovacs, K., Vértes, A. 2009. Jarosite inclusion of fluoride and its potential significance to bioleaching of sulphide minerals Hydrometallurgy. 96 108-116.

[28] Márquez, M.A.G. 1999. Mineralogia dos processos de oxidacao sobre pressao e bacteriana do minerio de ouro da mina Sao Bento, MG. Tese de doutorado. Universidad de Brasilia.

[29] Xuguang, S. 2005. The investigation of chemical structure of coal macerals via transmitted-light FT-IR microspectroscopy. Spectrochimica Acta Part A: Molecular and Biomolecular Spectroscopy. 62 557.

[30] Naumann, D., Helm, D. 1995. FEMS Microbiology Letters. 126 75

[31] Parker, A., Klauber, C., Kougianos, A., Waltling, H.R., Van Bronswijk, W. 2003. An x-ray photoelectron spectroscopy study of the mechanism of chalcopyrite leaching. Hydrometallurgy. 71(1–2), 265–276.

[32] Sharma, P.K., Hanumantha, R. K. 2005. Miner. Metal. Process. 22 31

[33] Xia L., Liu J., Xiao L., Zeng J., Li B., Geng M. and Qiu G. 2008. Single and cooperative bioleaching of sphalerite by two kinds of bacteria—*Acidithiobacillus ferriooxidans* and *Acidithiobacillus thiooxidans*. Trans. Nonferrous Met. Soc. China. 12 190

[34] Sandström, Å., Shchukarev, A., Jan Paul. 2005. XPS characterisation of chalcopyrite chemically and bio-leached at high and low redox potential. Minerals Engineering. 18 505–515.

[35] Mejía, E.R., Ospina, J.D., Márquez M.A., Morales, A.L. 2009. Oxidation of chalcopyrite (CuFeS2) by Acidithiobacillus ferrooxidansand a mixed culture of *Acidithiobacillus ferrooxidans andAcidithiobacillus thiooxidans* like bacterium in shake flasksAdvanced Materials Research. 71-73. 385-388.

[36] Schippers, A. 2007. Microorganisms involved in bioleaching and nucleic acid-based molecular methods for their identification and quantification. Microbial Processing of Metal Sílfides. Chapter one. Eddited by Edgardo R. Donati & Wolfgang Sand. Springer.

[37] Shrihari, R.K., Gandhi, K.S., Natarajan, K.A. 1991. Role of cell attachment in leaching of chalcopyrite mineral by Thiobacillus ferrooxidans. Applied Microbiology and Biotechnology. 36 278-282.

[38] A. Akcil, H. Ciftci, H. Deveci. 2007. Mineral Engineering. 20 310

[39] Cardona I.C. 2008. Mineralogía del proceso de biodesulfurización de carbones provenientes de la zona río Aguachinte – río Asnazú (valle del cauca y cauca). Tesis de Maestría. Universidad Nacional de Colombia, sede Medellín.

[40] Ivarson, K.C., Ross, G.J., Miles, N.M. 1979. The microbiological formation of basic ferric sulfates: II. Crystallization in presence of potassium, ammonium, and sodium-salts. Soil Science Society of America Journal, 43 (1979), 908–912.

[41] Jiang, T., Li, Q., Yang Y., Li, G., Qiu, G. 2008. Bio-oxidation of arsenopyrite. Trans. Nonferrous Met. Soc. China. 18. 1433–1438.

[42] Urbano, G., Meléndez, A.M., Reyes, V.E., Veloz, M.A., Gonzáles, I. 2007. Galvanic interactions between galena – sphalerite and their reactivity. International Journal of Mineral Processing. 82 148 – 155.

[43] Gahana, C.S., Sundkvista, J.; Sandströma, Åke. 2009. A study on the toxic effects of chloride on the biooxidation efficiency of pyrite. Journal of Hazardous Materials. 172 1273–1281.

[44] Hiroyoshi N., Hirota M., Hirajima T., Tsunekawa M. 1997. A case of ferrous sulfate addition enhancing chalcopyrite leaching. Hydrometallurgy. 47 37-45.

[45] Hiroyoshi, N., Arai, M., Miki, H., Tsunekawa, M., Hirajima, T. 2002. A new reaction model for the catalytic effect of silver ions on chalcopyrite leaching in sulfuric acid solution. Hydrometallurgy. 63 257-267

[46] Hiroyoshi, N., Kitagawa, H., Tsunekawa, M. 2008. Effect of solution composition on the optimum redox potential for chalcopyrite leaching in sulfuric acid solution. Hydrometallurgy. 91 144-149.

[47] Hiroyoshi, N., Miki, H., Hirajima, T., Hirajima, T., Tsunekawa, M. 2001. Enhancement of chalcopyrite leaching by ferrous ion in acid ferric sulfate solution. Hydrometallurgy. 60 185-197

[48] Shrihari, J.J.M., Kumar, R., Gandhi, K.S. 1995. Dissolution of particles of pyrite mineral by direct attachment of Thiobacillus ferrooxidans. Hydrometallurgy. 38(2) 175-187.

IntechOpen

IntechOpen

IntechOpen